Journal of Human Evolution 57 (2009) 465–483

Contents lists available at ScienceDirect

Journal of Human Evolution

journal homepage: www.elsevier.com/locate/jhevol

Reconstructing the geomorphic history of Liang Bua, Flores, Indonesia: a stratigraphic interpretation of the occupational environment

K.E. Westaway [a,*], T. Sutikna [b], W.E. Saptomo [b], Jatmiko [b], M.J. Morwood [a,c], R.G. Roberts [a], D.R. Hobbs [a]

[a] GeoQuEST Research Centre, School of Earth and Environmental Sciences, University of Wollongong, Wollongong, NSW 2522, Australia
[b] Indonesian Centre for Archaeology, Jl. Raya Condet Pejaten No. 4, Jakarta 12001, Indonesia
[c] Archaeology and Palaeoanthropology, School of Human and Environmental Studies, University of New England, Armidale, New South Wales 2351, Australia

ARTICLE INFO

Article history:
Received 18 January 2008
Accepted 11 January 2009

Keywords:
Stratigraphy
Geomorphic history
Sedimentology
Geochronology
Environmental reconstruction

ABSTRACT

Liang Bua, in Flores, Indonesia, was formed as a subterranean chamber over 600 ka. From this time to the present, a series of geomorphic events influenced the structure of the cave and cave deposits, creating a complex stratigraphy. Within these deposits, nine main sedimentary units have been identified. The stratigraphic relationships between these units provide the evidence needed to reconstruct the geomorphic history of the cave. This history was dominated by water action, including slope wash processes, channel formation, pooling of water, and flowstone precipitation, which created waterfalls, cut-and-fill stratigraphy, large pools of water, and extensive flowstone cappings. The reconstructed sequence of events over the last 190 k.yr. has been summarized by a series of time slices that demonstrate the nature of the occupational environment in Liang Bua. The earliest artifacts at the site, dated to ~190 ka, testify to hominin presence in the area, but the reconstructions suggest that occupation of the cave itself may not have been possible until after ~100 ka. At ~95 ka, channel erosion of a basal unit, which displays evidence of deposition in a pond environment, created a greater relief on the cave floor, and formed remanent areas of higher ground that later became a focus for hominin occupation from 74–61 ka by the west wall and in the center of the cave, and from ~18–17 ka by the east wall. These zones have been identified according to the sloping nature of the stratigraphy and the distribution of artifacts, and their locations have implications for the archaeological interpretation of the site.

Introduction

Interpretations of site formation processes and the distribution of materials in archaeological sites fundamentally rely on an understanding of karstic and fluvial processes (Glover, 1979), and are limited by the stratigraphic integrity of the deposits and problems associated with establishing a chronology (Gilbertson et al., 2005). Excavations in Liang Bua, a large dissolution chamber situated 16 km from Ruteng in the mountainous Manggarai province of western Flores, have yielded a wealth of palaeoenvironmental, palaeontological, and archaeological evidence (Morwood et al., 2004, 2005, 2009; Westaway, 2006) contained within a complex stratigraphy. This evidence includes stone artifacts, plant and animal remains, pottery, metal items, skeletal remains of *Homo floresiensis* in the Pleistocene deposits, and modern humans in the Holocene (Morwood et al., 2004, 2005, 2009). The present study follows the recommendations of previous analyses of cave sites in this region (e.g., Glover, 1979; Anderson, 1997; Gilbertson et al., 2005) and provides a detailed geomorphological and chronological (Roberts et al., 2009) context for the interpretation of the materials excavated at Liang Bua.

Westaway et al. (2009a) discovered that Liang Bua is part of a much larger cave system, located within an extensive cone and basin topography, situated on the highest alluvial terrace (~30 m above the river) within a flight of at least five uplifted terraces (Westaway, 2006). Rapid uplift dictates the dominant geomorphological processes in this region, such as karst solution, alluvial downcutting, and surface wash erosion, all of which contributed to the formation, exposure, and development of Liang Bua. The influences of these processes can be observed in the cave's stratigraphic record, which contains sedimentary evidence for multiple geomorphological events. Interpreting the archaeological evidence requires an understanding of these processes, such as the mode of transport, the energy of the depositional environment, and an appreciation of their relative timing. In this paper we describe the stratigraphy, and its characteristics and sequential relationships, for

* Corresponding author.
E-mail address: kira@els.mq.edu.au (K.E. Westaway).

0047-2484/$ – see front matter © 2009 Elsevier Ltd. All rights reserved.
doi:10.1016/j.jhevol.2009.01.004

purposes of establishing a depositional history for the cave and identifying geomorphological events that have influenced the distribution of artifacts and skeletal remains.

Methods

In the field, we cleaned, illustrated, described, and sampled stratigraphic sections revealed by archaeological excavations. Subsequent analysis of a conglomerate deposit at the rear of the cave involved the excavation of small test pits to reveal the extent of deposition in the cave. We later extended an initial excavation, 1 m deep (CP1) and situated directly in front of the conglomerate wall, horizontally towards the center of the cave. We conducted two further excavations (50 cm^2 wide and ~2 m deep) in line with the original trench; one (CP3) located by the small stalagmite mound at the junction between the chambers, and the other (CP2) located between this and the original pit.

In the laboratory, we analyzed the range of particle sizes found in the cave samples using a Malvern Mastersizer 2600 to infer the mode of deposition (e.g., Chivas et al., 2001). The samples were thoroughly dried and sieved to 2000 μm to remove the larger grains, and a representative sample (~0.5 mg) was added until the laser obscuration was within range (between 10% and 20% obscuration). This sample was dispersed by both physical and ultrasonic agitation and the particle size distribution (in % volume) was plotted against particle size (in Phi units). We also analyzed sediment samples using a Philips (PWI 130/90) X-ray diffraction unit to determine the mineral composition of the sediments as an indication of provenance (e.g., Carr et al., 1999). In preparation, we ground the sediment into a fine powder using a pestle and mortar, and placed it into small aluminium trays. We scanned the samples from 4° to 70° (using a scan rate of 2°/min); the peaks were isolated using a peak analysis program, Traces 6 (e.g., Chivas et al., 2001).

Sedimentation and stratigraphy

The sediments in the cave can be divided into two areas: the rear chamber, comprising mainly of *in situ* and modified conglomerate and slope wash deposits, and the front chamber, consisting of deeply stratified and complex interbedded deposits (Fig. 1), with a ~10 m difference in height between the floor of the rear and front chambers (Westaway et al., 2009a). Excavations in Sectors I, III, and IV, near the center of the cave, and Sectors VII and XI, close to the easterly cave wall, revealed the structure of the deposits in the front chamber, which Morwood et al. (2009) describe in more detail, and reference will be made throughout to their four main stratigraphic figures (Morwood et al., 2009: Figures 10–12, 14). Further small-scale excavations also determined comparable information for the rear chamber using a series of small test pits, as described in the methods section.

Results

Correlation of the front and rear chambers produces a composite stratigraphy of nine main sedimentary units. In stratigraphic order, they consist of: 1) a conglomerate, 2) basal units, 3) collapse material, 4) an occupation level capped by flowstone, 5) channel deposits by the east wall of the cave, 6) a reworked and eroded conglomerate, 7) an occupation level containing the skeleton, 8) volcanic sediments, and 9) a younger occupational level and modern slope wash deposits (Fig. 2). The extent and elevation of these units are illustrated in the cross sectional profile of the cave (Fig. 3), while the sedimentary characteristics (Table 1) and photographs (Fig. 4) of each unit have also been included. Not all of these units are found in each sector but, when chronologically combined, they reveal a sequence of geomorphological and sedimentological events that influenced the cave environment and its history of occupation.

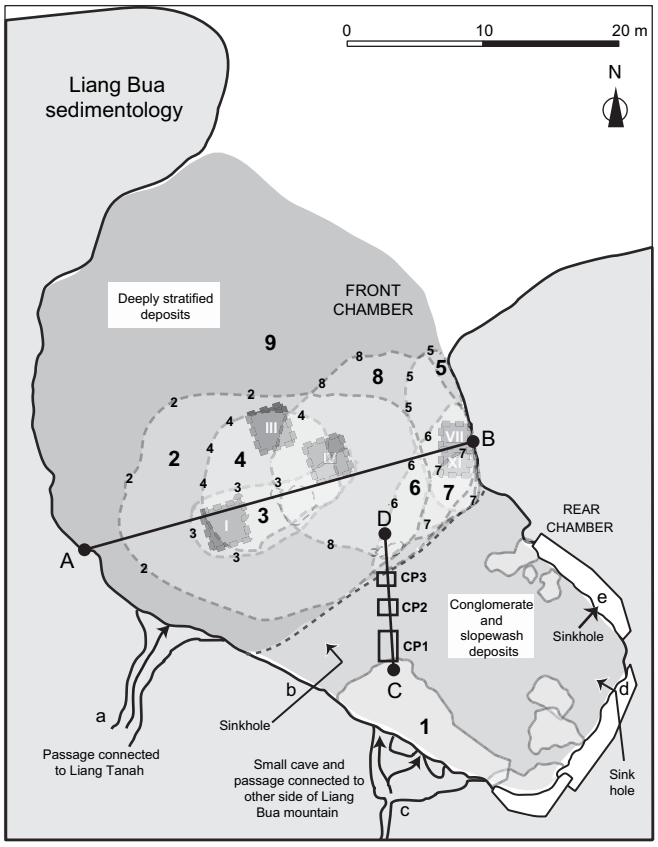

Figure 1. The structure and sedimentology of Liang Bua, showing the division of the cave into a rear and front chamber containing predominantly conglomerate and slope wash deposits, and deeply stratified deposits, respectively. The locations of the main excavations have been marked with dashed boxes (I, III, IV, VII, XI) and the smaller excavations (CP1, CP2, CP3) marked with solid boxes. The estimated extent of the main sedimentary units have been marked using dashed circles and numbered (1–9). A number of passages, sinkholes, and caves provide entry points into Liang Bua (a-e), and two transects running west to east (A–B) and south to north (C–D) provide the locations for the cross sections illustrated in Figs. 3 and 6, respectively.

Unit 1, conglomerate deposit

The structure, composition, and extent of the alluvial deposits at the rear of Liang Bua have been discussed in detail in Westaway et al. (2007, 2009a) so we include only a brief summary.

The Wae Racang River is, at present, ~30 m below and ~200 m from the cave entrance. However, the river previously occupied a similar elevation (~492 m.a.m.s.l.), as evidenced by a densely packed clast-supported conglomerate representing the river's first high-energy entry into the cave (Fig. 4a). In addition to this information, particle-size analysis of these deposits (Table 2 and Fig. 5) reveals a coarse matrix of silty sand that also indicates deposition by high-energy moving water. The combined clast and matrix size make this deposit one of the coarsest sedimentary units found in the cave. Lithological analysis of the dense framework of clasts reveals a predominantly volcanic composition of andesite, basalt, latite, trachytite, and dacite with occasional limestone, chert, and calcite clasts (Fig. 4a). This composition reflects the lithology of the bedrock throughout the course of the river, similar to the present composition of the Wae Racang riverbed. Both the extent of the

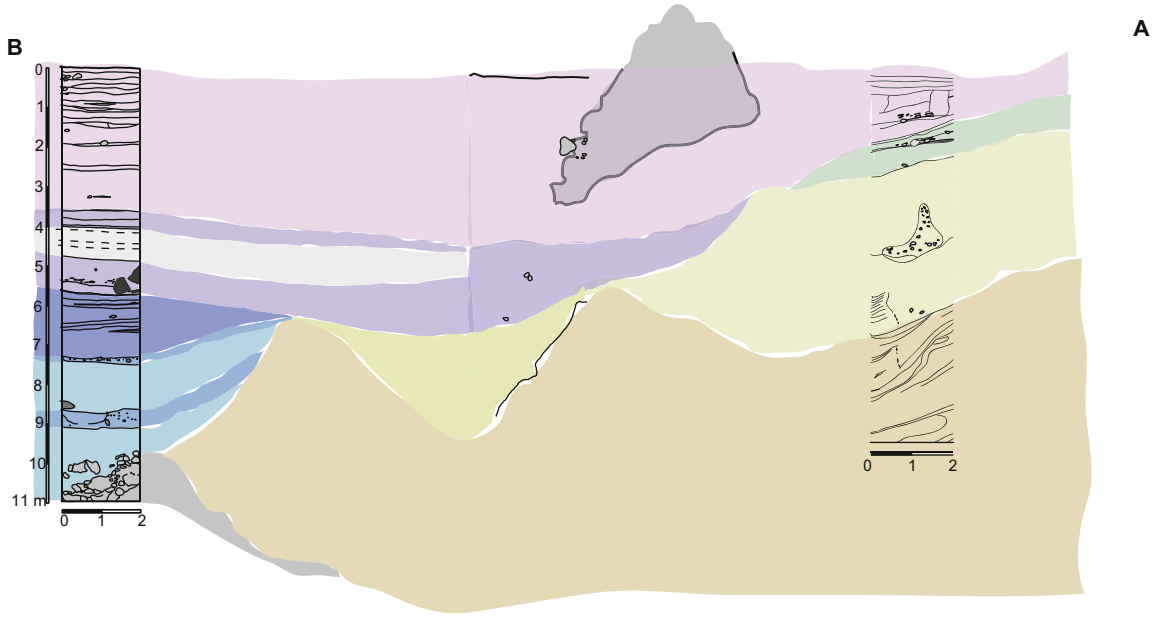

fallen pressure slabs resulting from the evolution of the domed cave roof. The presence of fine silts in this sedimentary unit, which may have been deposited in suspension (Table 2), indicates that the deep channels cut into the basal unit had subsequently filled with water and sediment. This pooling process may have been initiated by the presence of the large limestone blocks found in Sector IV, which effectively created a dam. The removal of this barrier caused the collapse material to slump within the scoured channel as seen in Sectors IV and III (Fig. 2).

The sedimentary conditions in Sector I also created a dam in this unit, which was caused by a deeply scoured channel. This channel infill contains evidence of slumping (Fig. 4c) but does not contain a similar amount of collapse material, as found in Sector IV. When compared with the elevation of the channel in Sector IV (Fig. 3), this channel represents stratigraphically higher ground that caused the larger collapse material to slump into the lower-lying topography in the center of the cave.

Unit 4, occupation level capped by flowstone

Silty clay deposits overlie the collapse material and represent the second main layer of occupation. They occur in Sectors I and III, and most extensively in Sector IV. Previous occupation may have occurred, but phases of earlier channel formation would have removed such evidence. Fine silts and clays comprise this unit (Table 2, Layer 8c), with high concentrations of gravel, stone artifacts, and bone, including those of neonatal *Stegodon*, giant tortoise, and *Homo* (Fig. 4e). It is composed predominantly of clays and volcanic glass, with traces of charcoal from either anthropogenic fires inside the cave, or from natural fires outside (Table 3, Layer 8c). The glass shards may have been reworked from volcanic material deposited close to the cave, while the presence of kaolinite and chlorite may have been derived from the soils outside the cave or may indicate that this unit has undergone extensive pre- or post-depositional weathering. The concentration and distribution of archaeological material in Sector IV, along with the sloping nature of this unit, suggest that these artifacts have slipped slightly from the higher levels in the southwest corner of this sector. However, the presence of conjoin sets of flakes confirms that they have moved no more than 1–2 m (Moore et al., 2009). The presence of thin layers of flowstone capping the deposit and interspersed within, confirms that water has been consistently flowing from this higher ground, and offers a potential agency for the accumulation of archaeological material in Sector IV. In Sector I, the unit has been capped by a flowstone and is situated at a much higher stratigraphic level. The difference in elevation confirms that this area represented relatively higher ground throughout the development of the cave (Fig. 3). The maximum thickness of the unit ranges from

Table 1
Sedimentary characteristics of the nine main units.

Unit	Sedimentary Classification – mean particle size (μm)	Average thickness (m)	Extent	Color	Sedimentary structure	LBC	Clasts	Sorting[a]	Roundness[b]	Composition	Dip (° and direction)	Variability	Fossils	Archaeology	Diagenetic/ changes reworking	Summary	Location key Sectors
1 Conglomerate	Gravel (clast supported) matrix silty sand - 134	~6	Rear cave	10 yr 5/4	Massive with some fining upwards	Sharp	Y	2.0	0.8	Meta / Volcanic limestone	9 NW	Variable coarse and fine	None	Stone tools	Eroded reworked	High energy alluvial deposit	CP1-3
2 Basal	Silty clay with lenses of iron oxide and sand (matrix supported) - 9	4–5	Front cave	10 yr 5/3	Low angle cross / non parallel convoluted bedding	?	N	–	–	–	20–45 S	Homogenous	Sterile	None	Convoluted	Silty basal suspension deposit	I, III, IV
3 Collapse	Silty clay matrix (matrix supported) - 138	2.5–3	Center cave	10 yr 5/3	Massive	Sharp	Y	1.0	0.4	Limestone blocks (>4 m)	45 E	Homogenous	Bone - high densities	Stone tools (high densities)	Slumping and compaction	Clayey suspension deposit cont. collapse material	I, IV
4 Occupation	Silty clay (matrix supported) - 22	1–2	Center cave	10 yr 6/3	Parallel bedding layered by flowstones	Sharp	Y	0.5	0.5	Meta / Volcanic limestone	–	Homogenous	Bone: *Stegodon* hominins	Stone tools	–	Massive silty clay containing occupation evidence	I, III, IV
5 Channel	Clayey silt (matrix supported)- 14	1.5–2	East wall	10 yr 4/4	Massive	Diffuse	N	–	–	Limestone	30 N	Homogenous	Bone	Stone tools hearth	–	Silty suspension deposit	VII/XI
6 Eroded / Reworked Conglomerate	Gravel clasts / clayey silt matrix (clast supported)- 33	0.5	East wall	10 yr 4/4	Massive	Sharp	Y	0.5	0.8	Meta / Volcanic	30 N	Variable	Sterile	Stone tools	Reworked matrix and clasts	Reworked conglomerate unit	VII/XI
7 Skeleton level	Clayey silt (matrix supported) - 8	1.5–2	East wall	10 yr 3/4	Massive	Sharp	Y	0.5	0.8	Limestone	30 N	Homogenous	Bone - high densities	Stone tools hearth	–	Massive silty deposits cont. extensive occupation	VII/XI
8 Volcanic	Fine silts / sandy silts (matrix supported) – 143-20	2.5–3	East wall / center cave	2.5 y 4/3 6/2	Laminations /loading structures/ massive	Diffuse/ very sharp	N	–	–	–	30 N	Variable many diff units	Sterile	None	Loading and lenses reworked	Primary and reworked volcanically derived deposits	III, IV, VII/XI
9 Younger occupation	Clayey silts / sandy silts (matrix supported)- 35	2.5–4	Front cave / rear cave	10 yr 3/3	Horizontal bedding	Diffuse	Y	1.0	0.3	Limestone	–	Homogenous	Bone	Stone metal tools burials pottery beads	–	Horizontally lain silts by sheetwash	I, III, IV, VII/XI

[a] Sorting classification based on Gardiner and Dackombe (1983): <0.35 very well sorted, 0.35–0.50 well sorted, 0.50–1.0 moderately sorted, 1.0–2.0 poorly sorted, <2.0 very poorly sorted.
[b] Particle roundness based on Gardiner and Dackombe (1983) ranging from 0.1: angular to 0.9: round.

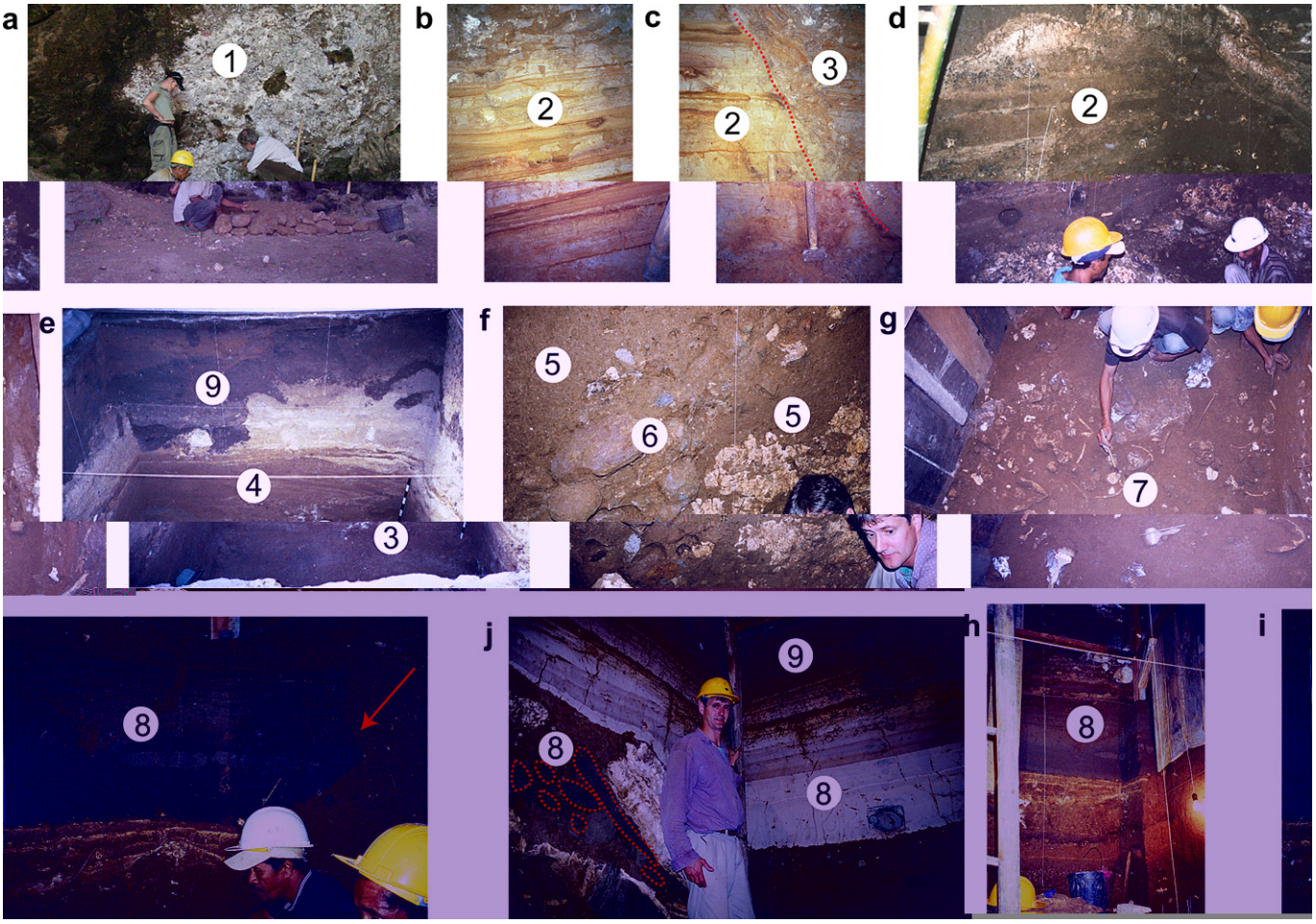

Figure 4. Photographs of the nine main sedimentary units. The photographs were taken in the following locations: (a) excavations by the conglomerate at the rear of the cave; (b) and (c) the base of Sector I; (d) the base of Sector IV; (e) the top of Sector I; (f) the base of Sector VII; (g) Sector XI; (h) and (i) towards the top of Sector XI; and (j) towards the base of Sector IV. The numbered circles refer to each of the nine units as illustrated in Fig. 2. The dotted red line in (c) signifies the erosion contact in Sector I, the red arrow in (i) points to the vertical erosion contact in the original BTS deposit in Sector XI, while the dotted lines in (j) highlight the lenses of BTS in Sector IV.

only 1 m in Sectors I and III, to 2 m in Sector IV, but has been heavily dissected on the northern and eastern edges of Sector IV, the easterly end of Sector III, and the south-easterly corner of Sector I by additional channel erosion (Morwood et al., 2009). Flowstone capping protected another area of higher ground in the southern and western side of this deposit in Sector IV.

Unit 5, channel deposits by the east wall

Unit 2 sediments at the base of Sectors I, III, and IV imply that a pond covered the entire cave floor. In contrast, this unit is absent from the base of Sectors VII and XI (Fig. 3), suggesting its complete erosion from the East wall location by the formation of a wide and deep channel. This wide channel was later filled to a thickness of 2 m with a fine clayey silt suspension deposit (Fig. 4f, Table 2, Layers X and T). The deposit was interspersed with rockfall and large (1–2 m) limestone slabs that may have acted as a dam, and given that this unit is not present in the center of the cave, it may represent localized deposition within a pool. The by-products of weathered volcanic minerals and reworked soils dominate these sediments, along with small quantities of quartz eroded from local volcanic units (Table 3, Layer X). While representing a stratigraphically younger deposit than the basal sediments, the depth and degree of water saturation in this unit suggests that the majority of weathering occurred within the cave environment.

Unit 6, eroded and reworked conglomerate

Eroded and reworked conglomerate occur in the easterly corner of the rear and front chambers (Fig. 1). The location of these deposits confirms that this unit formerly extended across the entire rear section of the cave, and then subsequently eroded and transported into the front chamber. Additional evidence for this erosion can been observed on the east-facing wall of the conglomerate cliff, where large sections of the wall have been removed, causing it to slope inwards and form small scree slopes. The north-facing wall has been severely undercut, creating a substantial overhang, which towers over a deep channel found 1.2 m below slope wash deposits. Slope wash processes, such as sheet wash, rill wash, and overland flow, originate from the large sinkhole situated directly above this eroded area, and cause the down slope movement of sediment by mass movement processes, such as slide, slump, creep, and slip. These processes have played a major role in modifying the original deposit.

The deposition of this unit in Sector VII (Fig. 4f) may have occurred during one large mass movement event, possibly during a storm. Additional evidence for slope wash activity can be seen in the extensive deposits (up to 5 m thick) at the southerly end of the cave,

Table 2
Particle size analysis of selected layers from the Liang Bua stratigraphy. The bracketed number after the layer code refers to one of the nine sedimentary units described in the text and illustrated in Fig. 2.

Sector	Layer (Unit)	Lithology	Mean (μm)	Mode (μm)	Median (μm)	Interpretation[d]
Con	Basal **(1)**	Silty sand	134	450	42	Fluvial bedload deposit, high energy environment, e.g., deposited by high-energy moving water, this unit represents the coarsest material in found in the cave
IV	12 **(2)**	Silt	9	21	6	Suspended load, low energy environment, e.g., deposited by suspension in body of standing water, possibly a pool
IV	9 **(3)**	Clayey silt	138	78	65	Intermittently suspended load, low to medium energy environment, e.g., emplaced by a channel but deposited by suspension
IV	8c **(4)**	Clayey silt	22	42	15	Suspended load, low energy environment, e.g., deposited by suspension in a pool of standing water
VII	X **(5)**	Clayey silt	14	20	9	Suspended load, low energy environment, e.g., deposited by suspension in a pool of standing water with no movement
VII	T **(5)**	Clayey silt	14	28	9	Suspended load, low energy environment, e.g., deposited by suspension in a pool of standing water
VII	S **(6)**	Sandy silt	33	16	10	Suspended load, low to medium energy environment, e.g., suggests some moving water but with some suspension
VII	R **(7)**	Clayey silt	8	15	5	Suspended load, low energy environment, e.g., deposited by suspension in a pool with little movement
IV	6 **(8)**	Silty sand	165	125	57	Bedload, high energy environment, e.g., deposited in moving water, possibly a channel
XI	BTS[a] **(8)**	Silty sand	143	127	104	Bedload, high energy environment, e.g., deposited in a fairly fast moving channel with erosive capabilities
VII	O **(8)**	Clayey silt	41	60	16	Suspended load, low energy environment, e.g., deposited by suspension with some water movement
VII	BTSl[b] **(8)**	Silty sand	89	161	62	Bedload, high energy environment, e.g., deposited in moving water channel with no suspension
VII	Nd[c] **(8)**	Sandy silt	60	57	32	Intermittently suspended load, low to medium energy environment, e.g., some degree of gently moving water, mostly suspension
VII	Nc[c] **(8)**	Silt	28	49	23	Suspended load, low energy environment, e.g., deposited by suspension in a pool of standing water
VII	Nb[c] **(8)**	Silt	33	50	28	Suspended load, low energy environment, e.g., deposited by suspension in a pool of standing water
VII	Na[c] **(8)**	Silt	20	38	16	Suspended load, low energy environment, e.g., deposited by suspension in a pool of standing water
IV	4 **(9)**	Clayey silt	35	48	13	Suspended load, low energy environment, e.g., deposited in slightly moving water with later suspension
IV	1i **(9)**	Clayey silt	21	31	12	Suspended load, low energy environment, e.g., deposited in slightly moving water with later suspension
VII	G **(9)**	Sandy silt	102	28	31	Suspended load, low to medium energy environment, e.g., deposited in channel of water with erosive and depositional abilities
VII	D **(9)**	Silt	39	30	22	Suspended load, low energy environment, e.g., deposited in gently moving water

[a] BTS refers to black tuffaceous sand unit.
[b] BTSl refers to black tuffaceous sand lens.
[c] Layers Na–Nd represent the white tuffaceous silts (WTS).
[d] Bedload, intermittently suspended load, and suspended load determined by modal grain size according to Bridge (2003).

which partly bury the conglomerate, and in a path of water that periodically emerged from the sinkhole, as depicted by moss staining.

Excavations directly in front of, and perpendicular to, the north-facing conglomerate wall (CP1, CP2, and CP3, location of transect marked as C–D on Fig. 1) suggest that the deposit has been extensively modified since its initial deposition (Fig. 6). The remains of the *in situ* deposit, now buried under slope wash deposits, extend for another 7.7 m towards a small stalagmite mound situated at the junction between the two chambers. This extent suggests that the conglomerate previously reached a similar height as the top of the present cliff, and was subsequently eroded when the overhang was formed. The stratigraphy in these excavations (Fig. 6) revealed that slope wash deposits overlie a thick accumulation of cemented gravel. Thin flowstone layers (at 1.25 m in CP2 and at 1.86 m in CP3) cap the eroded conglomerate deposit, which is found between 1.36–1.88 m in depth. As the flowstone deposits post-date this erosional event, they have been constrained by U-series techniques to provide a minimum age for the conclusion of erosion and the beginning of sediment accumulation. However, the actual depth of the conglomerate deposit, lithology of the lower bedding contact, and form of the bedrock contact (i.e., sloping or flat) were not encountered during excavation and are, therefore, unknown.

A large section of the reworked conglomerate occurs at the base of Sectors VII/XI (Layers S and V, Fig. 4f). It contains a similar clast size and composition as the *in situ* conglomerate deposit, but a slightly finer composition (sandy silt). This suggests that the final emplacement of the matrix was by suspension in the pool by the east wall, where it combined with the finer pool deposits. This unit was deposited in two separate phases, which sandwich a clayey silt suspension deposit and slope down towards the northern edge of Sector VII. The stratigraphy at this elevation implies that higher ground previously existed towards the south of the sector, and a pool formed towards the north.

Unit 7, occupation level containing the skeleton

Another clayey-silt suspension deposit overlies the second phase of reworked conglomerate in Sector VII, and contains a further phase of intensive occupation. This unit, up to 1.5 m thick, represents a pool deposit and is found only in the sectors that abut the easterly cave wall. It is almost sterile of archaeological evidence, with the notable exception of the almost complete LB1 skeleton (holotype of *Homo floresiensis*). In contrast, deposits found to the south of the skeleton represent the pool bank and contain stone artifacts, charcoal, and bone, including *Stegodon*, Komodo dragon,

and other hominin remains (Fig. 4g). Also found in this unit were a series of seven burnt dacitic stones arranged in a hearth formation (Morwood et al., 2005). These bank and pool deposits are composed of clays, minerals that form on basalts, and glass shards of unknown origin (Table 3, Layer R). It is possible that the clays

Table 3
X-ray diffraction analysis of selected layers from the Liang Bua stratigraphy. The number in brackets after the Layer code refers to one of the nine sedimentary units described in the text and illustrated in Fig. 2. Minerals followed by a question mark indicate that their presence is uncertain.

Sector	Layer (Unit)	Components	Most likely origin
IV	9 **(3)**	Montmorillonite	Clay, derived from the weathering of volcanic minerals
		Magnesiohornblende	Eroded from volcanic material, a primary volcanic mineral
		Quartz	Not a primary volcanic mineral in a basaltic environment, but a secondary mineral found in small quantities in infilling vesicles or veins
		Anorthite	Plagioclase feldspar, primary volcanic mineral
		Maghemite	Derived from the weathering of volcanic minerals
IV	8c **(4)**	Kaolinite	Clay from weathering of silicate minerals
		Quartz	Not a primary volcanic mineral in a basaltic environment, but a secondary mineral found in small quantities in infilling vesicles or veins
		Chlorite	Derived from the breakdown of mafic minerals, e.g., olivine and pyroxene
		Carbon?	Charcoal fragments derived from fire (anthropogenic/natural)
		Glass shards?	Tephra deposit, possibly from an earlier volcanic eruption
VII	X **(5)**	Smectite	Clay, derived from weathering
		Geothite	Hydrated iron oxide produced by the weathering of iron minerals
		Quartz	Not a primary volcanic mineral in a basaltic environment, but a secondary mineral found in small quantities in infilling vesicles or veins
		Illite	Clay, a weathering product
VII	R **(7)**	Kaolinite	Clay, derived from the weathering of feldspars
		Heulandite	A primary volcanic mineral formed in cavities in basalt
		Glass shards?	From a tephra - possibly from an earlier volcanic eruption
XI	BTS **(8)**	Labradorite	Plagioclase-feldspar, a primary volcanic mineral found in basalt
		Hornblende	A dark amphibole, common in igneous and metamorphic rocks, constituent of basalt
		Orthopyroxene	Rock forming silicate mineral found in igneous rocks, present in volcanic lavas
		Magnetite	Iron oxide ferrimagnetic mineral found in igneous rocks and magma
		Quartz	Not a primary volcanic mineral in a basaltic environment, but a secondary mineral found in small quantities in infilling vesicles or veins
		Chlorite	Derived from the breakdown of mafic minerals, e.g., orthopyroxene
XI	B **(9)**	Anorthite	Calcium rich plagioclase feldspar, primary volcanic mineral
		Halloysite	Clay derived from the leaching of water through volcanic rocks
		Potassium feldspar	A primary volcanic mineral, abundant in volcanic environments but susceptible to weathering and reduced down to clays
		Actinolite	A primary volcanic mineral that has been altered, possibly by hydrothermal processes (an altered hornblende)
VII	G **(9)**	Calcite	Carbonate mineral possibly eroded from the Waihekang formation
		Kaolinite	Clay, derived from the weathering of feldspars
		Gypsum	A secondary mineral formed on the cave wall prior to deposition or derived from bat guano
		Carbon	Charcoal fragments derived from anthropogenic or natural fires

et al., 2009a). In addition, the presence of clays and minerals eroded from local volcanic rocks suggests that the source area for these sediments was localized, and probably contained within the catchment of the Wae Racang. This localized sedimentary origin was maintained throughout the deposition of the main units, apart from the introduction of small amounts volcanic glass shards in Units 4 and 7, and the deposition of the volcanic silts (Turney, pers. comm.).

Chronological results

The age range of these complex interbedded units, established by a program of extensive dating presented in Roberts et al. (2009), will enable the interpretation of this stratigraphic evidence. Using the results of the dating techniques (luminescence: red TL, blue IRSL, and OSL; U-series, ESR/U-series combined, and radiocarbon) presented in Table 4 (with methods and supporting information in Roberts et al., 2009), a chronology for the nine sedimentary units has been established, and is presented in Table 5. All sample codes refer to dating results found in Table 4 unless otherwise stated.

Discussion

Identifying the main geomorphic events in Liang Bua

The previous description of the main sedimentary units illustrates the role played by water action in determining the sedimentation of the cave. From this analysis, five main processes relating to water action have been discerned that occurred in specific areas in the cave. These processes determined the nature of the cave deposits in these locations, and influenced human occupational activities. They are as follows: slope wash processes, channel formation, pooling of water, flowstone precipitation, and post-depositional modifications.

Slope wash processes After the initial invasion by alluvium, slope wash processes dominated the areas around the sinkholes, modified the sediments, and determined the nature of the sedimentation up to the present-day. These slope wash waters originated from the three source sinkholes and a cave located in the west wall, as illustrated in Fig. 1. For example, these processes filled eroded channels (e.g., Sector VII) and eroded pool deposits (e.g., Sector XI). We speculate that the modifications to the conglomerate deposit by either erosion (e.g., the removal of conglomerate from between the west and east cave walls) or deposition (e.g., the redeposition of the conglomerate in the sectors) were dependent on changes to the hydrology associated with the source sinkholes and the severity of the monsoonal seasons. This implies that a strong link existed between storms/persistent wet seasons, and deposition/reworking in the cave environment (Westaway et al., 2009b).

Channel formation The presence of erosional contacts found in the sediments of Sectors I, III, and IV demonstrate the influence of channel erosion on the evolution of the cave. During the main

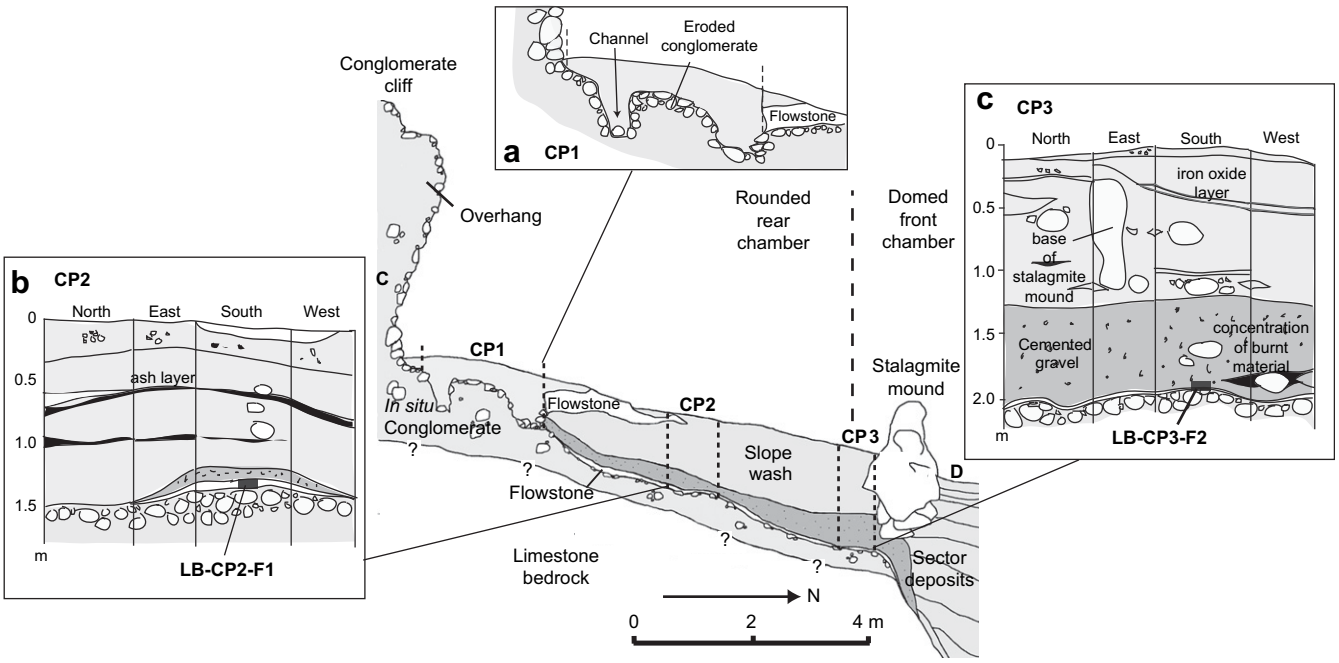

Figure 6. The sedimentary structure of the remnant *in situ* conglomerate deposit, from the conglomerate cliff to the stalagmite at the junction between the two chambers, according to the stratigraphy of three small excavations, CP1 (a), CP2 (b), and CP3 (c). This structure has been illustrated as a cross-section of the transect C–D depicted in Fig. 1. Erosion of the original conglomerate created the overhang and deep channel (a). The stratigraphic relationship between the flowstone cover, cemented gravel (dark shading), and slope wash sediments (mid-shading) was determined by an analysis of the excavation sediments. The location of the flowstones sampled for U-series dating are shown as filled rectangles, and the vertical dashed line marks the boundary between the front and rear chambers. The contact between the *in situ* conglomerate and the limestone bedrock was not encountered during excavation, so this boundary has been estimated and subsequently marked accordingly (question marks).

phases of channel formation, the size of the channels and the creation of an uneven cave floor surface would have made the cave difficult to occupy. In a similar manner to the slope wash processes, the size of these channels may have been directly influenced by the amount of water passing through the landscape. Thus, according to the pattern seen in the present-day cave systems, severe monsoonal seasons would have resulted in large channels, and drier seasons would have caused either a reduction in the size and constancy of the channels or resulted in ephemeral streams that were activated by intermittent storms. The initiation of these channels in the basal units of the cave created relief in specific locations (discussed in the section below on basal cave sediments) that persisted throughout the occupation period. The presence of a large stalagmite mound to the south of Sector IV agrees with the suggested pattern of relief, as the calcite accumulated in this protected location a few meters above the erosive effects of the channels.

Pooling of water The presence of fine suspension deposits throughout the stratigraphy indicates that the pooling of water is also a major process within specific locations in the cave environment. From the composite stratigraphy, five main pooling events have been identified: 1) prior to the exposure of the cave; 2) after the river first entered the cave; 3) during the occupation period that was later capped by a flowstone; 4) during the sedimentary infilling of the channels close to the easterly cave wall; and 5) during the volcanic eruption period that deposited the white tephra bearing silts.

The occurrence of pooling at certain points in the stratigraphic column could either be a function of the sedimentary regime (e.g., the presence of collapse material creating a dam effect) or the climate (e.g., during drier periods the source water flow decreased causing channels to be abandoned to form shallow pools). During phases of heavier monsoon, these pools received influxes of much coarser material and the increased water flow may have caused them to revert back into channels. After these wetter events, residual water trapped in channel depressions, or dams created by collapse material, was periodically replenished by surface wash deposits. The location of the pools, situated stratigraphically above the channel deposits in Sectors IV and VII (Morwood et al., 2009: Figures 12 and 14, blue and red arrows, respectively) concurs with this interpretation.

The fine silts and clays found in the pools originate from four main areas: 1) the small passage (Fig. 1, "a") that links to Liang Tanah, a smaller cave located to the northwest of Liang Bua (Westaway et al., 2009a); 2) the passage connected to the small cave in the west wall (Fig. 1, "c"); 3) the erosion of silts and clays from the conglomerate matrix (Fig. 1, "1"); and 4) the sinkholes that channel slope wash and sediments into the rear of the cave (Fig. 1, "b" and "d"). The Liang Tanah passage lies along the west wall of the cave at a bearing of 275° (relative to true north) and can be identified by a profusion of flowstones, collapse material, ferns, and moss staining. The corresponding passage in Liang Tanah is situated at the rear of the cave at a slightly higher elevation than Liang Bua, and its location is confirmed by the presence of buried stalactites. As the entrance to this cave faces a steep mountainside (Golo Liang Tanah), it received large amounts of coarse sand and slope wash, which was then channelled into Liang Bua. Thick lenses of low-angled bedded coarse sand are found within the basal pond sediments of Sector I, close to the passage entrance into Liang Bua, suggesting that these units were deposited shortly after entering the cave. The relief in the passage may have promoted gravitational effects such as slumping, and aided their deposition.

Table 4
The luminescence and U-series dating results for the samples from Liang Bua. The supporting data for these ages can be found in Roberts et al. (2009).

Sample code	Sedimentary unit[a]	Dating technique[b]	Age (ka)[c]	Material dated
WR15	T	Red TL	118 ± 48	Sediment – quartz
LBC-37	1	Red TL	130 ± 57	Sediment – quartz
LBC-36	1	Red TL	193 ± 33	Sediment – quartz
LBS1-12	2	Red TL	55 ± 49	Sediment – quartz
LBS3-2	2	Red TL	106 ± 31	Sediment – quartz
LBS4-26	2	Red TL	65 ± 25	Sediment – quartz
LBS4-28	2	Red TL	110 ± 20	Sediment – quartz
LBS1-12	2	OSL	$87\ ^{+11}/_{-12}$	Sediment – quartz
LBS1-16	3	Red TL	52 ± 20	Sediment – quartz
LBS4-32	3	Red TL	95 ± 13	Sediment – quartz
LBS1-16	3	OSL	$75\ ^{+12}/_{-10}$	Sediment – quartz
LBS4-34	4	Red TL	70 ± 8	Sediment – quartz
LB-JR-6A/13-23	4	U-series	37.7 ± 0.2	Flowstone
LB-03-2/2-13	4	U-series	61.0 ± 2.4	Flowstone
LB-JR-8A	4	ESR/U-series	$74\ ^{+12}/_{-13}$	*Stegodon* tooth
LBS7-45	5	Red TL	55 ± 8	Sediment – quartz
LBS7-46	6	Red TL	41 ± 10	Sediment – quartz
LB-CP2-F1-B	6	U-series	48.5 ± 1.7	Flowstone
LB-CP2-F1-T	6	U-series	46.5 ± 0.5	Flowstone
LB-CP3-F2	6	U-series	46.3 ± 2.0	Flowstone
LBS7-40	7	Red TL	40 ± 8	Sediment – quartz
LBS7-42	7	Red TL	36 ± 5	Sediment – quartz
LBS7-40	7	Blue IRSL	14 ± 2	Sediment – feldspars
LBS7-42	7	Blue IRSL	6.8 ± 0.8	Sediment – feldspars
ANUA-27116	7	^{14}C	19.0–17.9	Charcoal
ANUA-27117	7	^{14}C	18.7–17.1	Charcoal
ANUA-19203	8	^{14}C	17.1–15.8	Charcoal
ANUA-27115	8	^{14}C	13.4–12.7	Charcoal
ANUA-23610	8	^{14}C	17.1–15.7	Charcoal
LBS4-30	8	Red TL	14 ± 3	Sediment – quartz
WK-16353	9	^{14}C	2.84–2.62	Charcoal
ANUA-19206	9	^{14}C	10.2–9.5	Charcoal
ANUA-19207	9	^{14}C	6.67–6.02	Charcoal
ANUA-19211	9	^{14}C	11.2–10.2	Charcoal

[a] T denotes a terrace sample, and the numbers 1–9 refer to the main sedimentary units in Fig. 2.
[b] Detailed methods for each technique are presented in Roberts et al. (2009).
[c] Supporting data for each technique are presented in Roberts et al. (2009).

Flowstone precipitation Throughout the sedimentary development of the cave, the precipitation of flowstones was a frequent occurrence. This precipitation ranged from large slabs of flowstone found within the basal sediment layers (e.g., sample LB-17A-2 3-8) and accumulations on eroded sections of the conglomerate (e.g., LB-CP2-F1), to recent accumulations on the present cave walls and floor. Flowstone precipitates on most surfaces within the cave environment, but as its formation signifies the presence of a constant film of flowing water, it predominantly occurs on sloping surfaces. Hence, the presence of sloping flowstone accumulations, with a necessary supply of flowing water, may indicate areas in the cave that would have been unsuitable for occupation.

Table 5
A chronology for the main sedimentary units in the cave, based on the results presented in Table 4 and Roberts et al. (2009).

Unit	Description	Age (ka)
9	The younger occupation level and modern slopewash	~11–3
8	Volcanic sediments	~16–11
7	The occupation level containing the skeleton	~18–16
6	The eroded and reworked conglomerate	~50–40
5	Channel sediments by east wall	~55–50
4	Occupation level capped by flowstone	~74–61
3	Collapse material	~100–95
2	Basal cave sediments	~130–100
1	Conglomerate	~190–130

Table 6
Average sedimentation rates for the sectors in Liang Bua using a combination of red TL dating, ^{14}C, U-series, and ESR/U-series combined (Roberts et al., 2009), since the sediments started to accumulate over a ~100 k.yr. period. Note: the rate for Sector I has been obscured by the erosion of the upper layers. Sector VII contains the fastest sedimentation, which represents the channel infill and sedimentary accumulation relating to the waterfall and pool feature by the east wall. The sectors within the center of the cave contain slightly lower rates, as they are not in the immediate vicinity of the sinkholes. The location of a pool just to the north of Sector XI provides an explanation for the slower rates in this Sector compared with Sector VII.

Sector	Average sedimentation rate (mm/ka)
I	63
III	275
IV	330
VII	487
XI	328

Post-depositional modifications Post-depositional subsidence can be observed in Unit 2, possibly due to erosion by sink or spring action. This process may have lowered the general level of this unit, but the bulk of the deposit remained intact and has maintained the original stratigraphic relationships with the overlying units. Unit 3 displays evidence of slumping and compaction due to the weight of the collapse material, and Unit 8 shows evidence of scour, deformation, and shallow lake water activity due to development of the tephra pool. The remaining Units 4, 5, 6, 7, and 9 display little evidence of post depositional modifications, and the processes outlined above (slope wash, channel formation, pooling, and flowstone precipitation) occurred only in specific areas of the cave, leaving a few locations that were later capped by flowstone precipitations or layers of conglomerate, relatively unaffected. This notion is supported by the mostly pristine and "as-struck" nature of the lithics in these locations, suggesting that this material had not been transported great distances (Moore et al., 2009). Furthermore, the stratigraphic integrity of some areas of the deposits is supported by sections that have remained completely undisturbed since deposition, e.g., Unit 4 in Sector I and IV, and Units 5, 6, and 7 at the base of Sector VII (Fig. 2).

Table 7
The average sedimentation rates for each of the nine main sedimentary units. The slowest sedimentation rate occurs during the deposition of the pond sediments, while the fastest occurs during the deposition of the pool deposits by the east wall. Note that there is no rate for the conglomerate unit as it was deposited in one depositional event and then subsequently reworked.

Unit	Description	Sedimentation rates (mm/ka)
9	The younger occupation level and modern slopewash	326
8	Volcanic sediments	428
7	The occupation level containing the skeleton	750
6	The eroded and reworked conglomerate	300
5	Channel sediments by east wall	200
4	Occupation level capped by flowstone	142
3	Collapse material	190
2	Basal cave sediments	70
1	Conglomerate	–

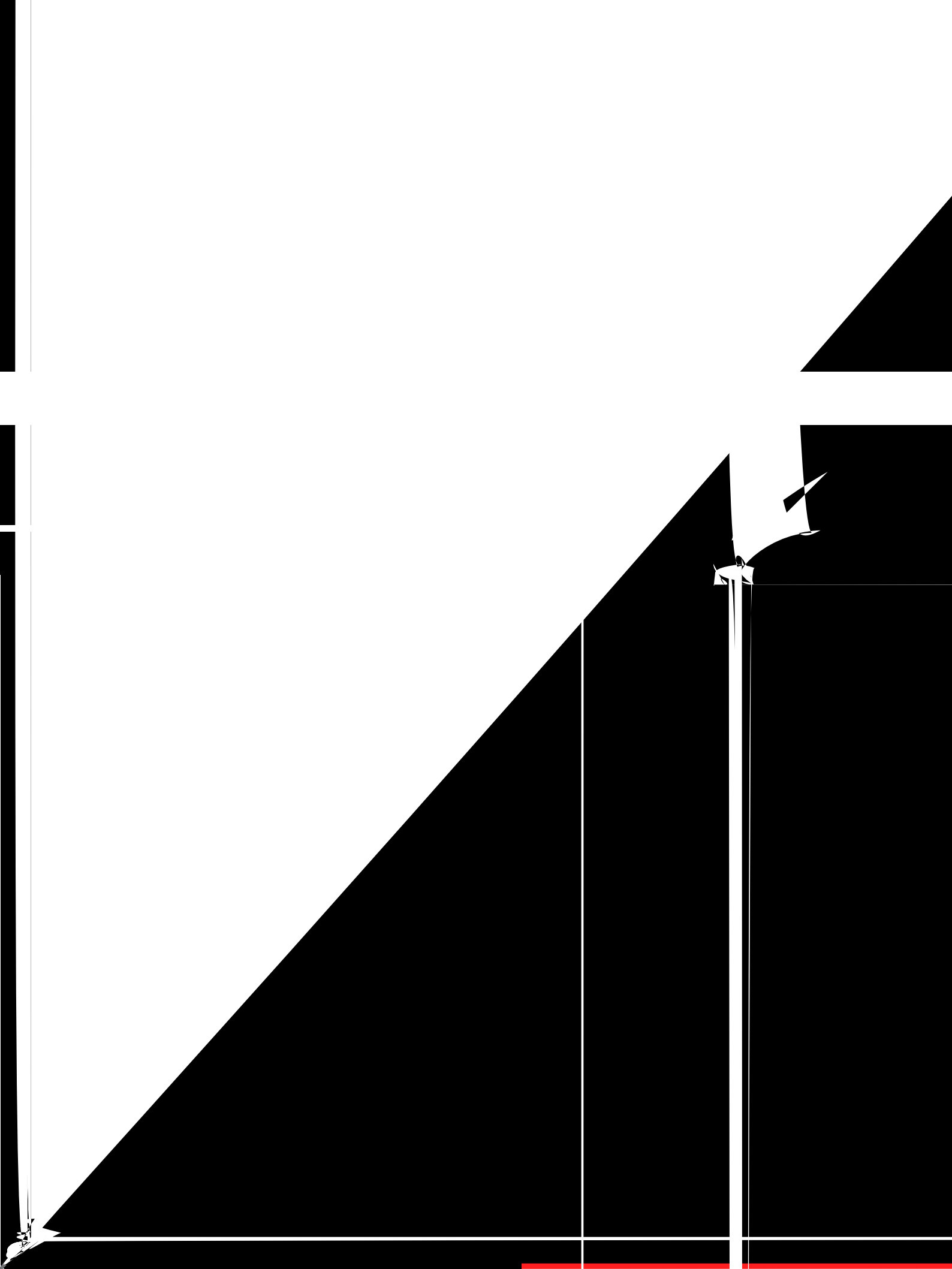

seen at the base of Sector I in the northwest corner and the southwest corner of Sector IV (Fig. 2a, c).

The basal cave sediments deposited at depths shallower than 8 m (Fig. 2), represented by ages of 106 ± 31 ka (sample LBS3-2), 110 ± 20 ka (sample LBS4-28), and 87 $^{+11}/_{-13}$ ka (sample LBS1-12, OSL result) produce a mean age of ~100 ka for both the red TL and OSL results, when the associated errors are taken into consideration. Sedimentary characteristics, such as finely laminated structures, imply that these silts and clays, derived from the Liang Tanah passage, were also deposited in a pond, which was contained by a rockfall dam at the entrance. However, the convoluted bedding (Fig. 4d) suggests that, at this time, water disturbances occurred, caused by river and slope wash water falling into the pond and a small degree of post-depositional subsidence. During large storm events, the river's tributary was able to breach the rockfall and rework this unit (Fig. 9), creating an uneven topography, laminations, and lenses of coarser material (Fig. 4b). Despite these post-depositional modifications, we are confident about the integrity of these burial ages (Roberts et al., 2009).

Presumably, these basal units once extended across the entire front chamber (Fig. 1), but prior to 55 ka, a large channel had formed by the east wall of the cave (Fig. 3), as suggested by the comparatively young age of 55 ± 8 ka (LBS7-45) for the Sector VII basal units. The location of this channel correlates with the extensive erosion of the conglomerate towards the east wall of the rear chamber, suggesting that a similar process was responsible for the erosion of both sedimentary units. Thus, the sedimentary and geomorphological evidence implies that surface wash from the rear sinkhole and west wall passage converged to create a large channel and produced extensive erosion on the easterly side of the cave.

At ~100 ka, the tributary had stopped entering the cave due to fluvial downcutting in the valley (Westaway et al., 2009a) and the majority of the pond water had drained from the front chamber, as implied by the presence of extensive channels within the former pond sediments (Morwood et al., 2009). A base level drop caused by this alluvial incision would have prevented water entering via the channel, and the remaining water may have been channelled through a newly formed sinkhole into the subterranean chamber below Liang Bua (Westaway et al., 2009a). Four main channels were operating during this time, issuing from the sinkhole at the rear of the cave, the sinkhole by the west wall above the eroded section of conglomerate cliff, a channel originating from the Liang Tanah passage that intersected the southeasterly corner of Sector III, and a channel originating from the cave in the west wall (Fig. 1). The extensive erosion of the original cave sediments, and then the basal unit by the river and channels, created an uneven topography in the fine silts and clays and caused a drop in elevation between the front and rear chambers (creating waterfalls by the east wall and center of the cave ~12 m in height). The channel originating from Liang Tanah formed a mass of water over the present location of Sector I. This accumulation of water may have persisted for at least 50 k.yr., as it was directly supplied with water from the neighbouring cave. These four channels may have coalesced at a central point within Liang Bua, as illustrated in Fig. 10.

The collapse material The deep channel formed in Unit 2 in Sector IV (Fig. 2) filled with collapse material and channel infill between 95 ± 13 ka (sample LBS4-32) and 131 ± 10 ka (sample LBS4-1, a maximum age). This age range supports the notion that the river had stopped entering the cave, and the ponding events had ceased by ~100 ka, as the age of the resulting channel infill suggests that the channel had been eroded prior to ~95 ka. It also suggests that these channel sediments are older than the occupation level capped by flowstone, and the relatively high density of archaeological evidence suggests that this sedimentary unit represents more than just ephemeral use of the cave, but rather represents the earliest phase of intensive occupation (Moore et al., 2009). The deep channel formed in Sector I was filled with a later accumulation of collapse material at ~75 ka (LBS1-16, OSL result), as discussed in the next section.

The occupation level capped by flowstone At ~70 ka, the erosion of the conglomerate was still occurring from flowing water originating from both sinkholes; the waterfalls (although reduced to a height of ~11 m) were still present by the east wall and center of the cave, and the four channels were still in operation (Fig. 11). The sedimentology of fine silts at this stratigraphic level implies that a small pool had formed over the top of Sectors III and IV, and ages of 69 ± 12 ka (sample LBS3-4) and 70 ± 8 ka (sample LBS4-34) for these sediments, respectively, supports this notion. The presence of thin flowstones within these deposits indicates that this pool occasionally became very shallow, allowing water to flow over the surface of the sediments.

Prior to this period, at 87 $^{+11}/_{-12}$ ka (LBS1-12), the pool over Sector I was accumulating fines via suspension with periodic influxes of coarser material. The later sediments represented deposition by a higher-energy regime, originating from the active Liang Tanah passage, which channelled water and sediments directly from Liang Tanah Mountain. The modal size of the coarsest grains indicates that the velocity of this channel had periodically increased since the deposition of the basal sediments, possibly

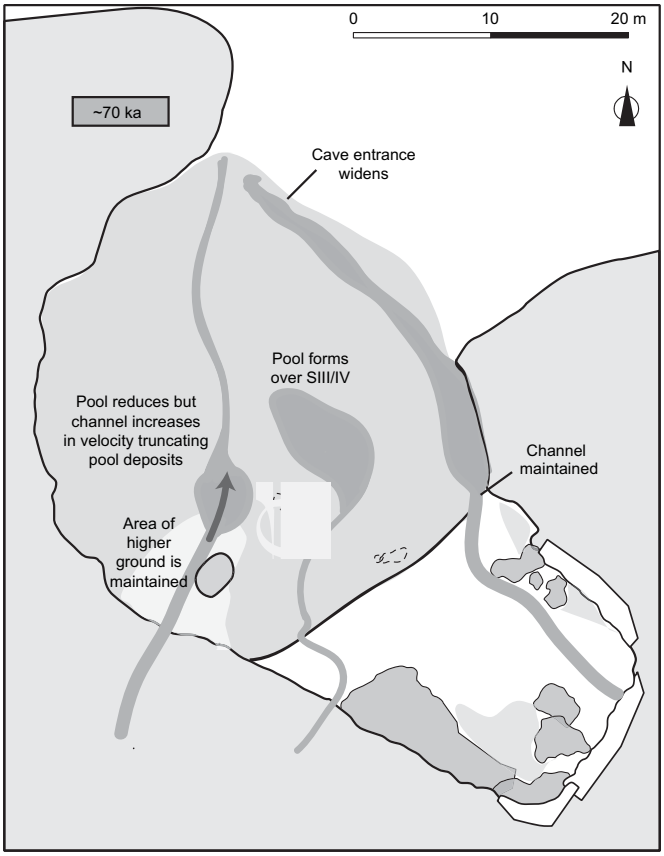

reflecting an increase in the severity of the monsoonal seasons. In contrast to the Sector IV pool, this water body may have been slightly deeper and less disturbed, which enabled the preservation of sedimentary structures. This deeper pool was severely truncated prior to 75 $^{+11}/_{-10}$ ka (sample LBS1-16), when the velocity of the channel originating from the Liang Tanah passage continued to increase, initiating large scouring episodes, which carved a deep erosion contact in the original basal units. This deep channel had rapidly filled with sediment and collapse material between 75 $^{+11}/_{-10}$ ka and 52 ± 20 ka (sample LBS1-16, OSL and red TL, respectively). The upper limit of the red TL age estimate is a more appropriate age, as these deposits were capped by a flowstone at ~61 ka (LB-03-2) and are thought to be older than the corresponding stratigraphic levels in Sectors III and IV, which contain sediments representing the second oldest occupation level at ~70–69 ka (LBS3-4 and LBS4-34, respectively).

The arrangement of pools and channels during this period almost surrounded an area of cave floor directly to the southwest of Sector IV (Fig. 10), which after a period of channel erosion may have created a greater relief and formed a remanent area of higher ground. This area is thought to have been a zone of occupation (Fig. 11) that represents the second intensive use of the cave by hominins, and may have been a source area for the occupational evidence found in the southern baulk of Sector IV. This higher ground may have been ~6 m above the base of the channel by the east wall and would have represented a flat, dry haven within the cave environment (free from channel erosion and surface wash) where occupational activities could take place. As Anderson (1997) argued that level floor areas are a feature of all occupied cave sites in Southeast Asia, it would appear that the development of these flat areas encouraged the occupation of the cave at this time. The 70–69 ka (LBS3-4 and LBS4-34) age range for the clayey silt deposits agrees with the 74 $^{+12}/_{-13}$ ka age (sample LB-JR-8A) for a *Stegodon* molar from the same elevation. In addition, the concentration of artifacts and *Stegodon* bones underneath the flowstone capping in Sector I (Morwood et al., 2009) suggests that another potential zone of occupation to the southwest corner of Sector I, may have existed between 75 ka (LBS1-16) and 61 ka (LB-03-2). This zone was located on an area of higher ground by the Liang Tanah passage, which persisted in the sediment column for at least ~90 k.yr. When this evidence is combined, this occupational level and sedimentary unit is effectively constrained to 74–61 ka (Tables 4 and 5).

An alternate explanation for the accumulation of archaeological material in these areas is that they represent zones of preservation that have not been affected by channel erosion or surface wash. This implies that occupation occurred throughout the cave but this evidence has only been preserved in certain areas. Without more detailed excavations it is difficult to determine the full extent of occupation. However, the persistence of the pool and channel sequence and pattern of relief in the stratigraphic column over a ~85 k.yr. period indicates that extensive occupation of the cave may have been difficult. Therefore, until further excavations are undertaken, this evidence, combined with the distribution of archaeological material in Sectors IV and VII/XI, supports the "higher ground" theory as a more likely explanation.

The channel deposits by the east wall The erosion of the conglomerate and sediments from the rear and front chambers had been reduced by ~50 ka, and the channel by the east wall had formed a pool that had started to accumulate fine suspension deposits at 55 ± 8 ka (sample LBS7-45). An absence of sedimentary structure in these deposits suggests that the rear sinkhole was disturbing the newly formed pool via the waterfall, which had been reduced to a height of ~9 m due to sedimentary infilling of the plunge pool (Fig. 12).

The sedimentology at this stratigraphic elevation suggests that slope wash processes fluctuated in magnitude but had not completely ceased, as sedimentary evidence for the maintenance of the three channels persists in the sediment column throughout this period. The sedimentological evidence of scouring over Sector IV suggests that the central channel, originating from the sinkhole by the west wall, had eroded the occupation deposits capped by flowstone leaving only the southwest corner unaffected. This scouring occurred after ~37 ka, as suggested by the age of the flowstone layers (sample LB-JR-6A) that accumulated over the southwest corner of Sector IV, protecting this area from erosion. A similar increase in flowstone precipitation occurred in the northwest corner of Sector I at ~61 ka (sample LB-03-2) and the southeast corner at ~53 ka (sample LB-03-1).

The eroded and reworked conglomerate The ages of the flowstones that cap the eroded conglomerate section by the west wall (samples LB-CP2-F1 and LB-CP3-F2) suggest that after 49 ka, the erosion of this unit had ceased. But the source sinkhole was still supplying this area with water via sheetwash flow that enabled flowstone precipitation (Fig. 12).

An influx of reworked conglomerate from the rear chamber was deposited into the newly formed pool between 55–41 ka (samples LBS7-45 and LBS7-46, respectively). This influx may reflect an

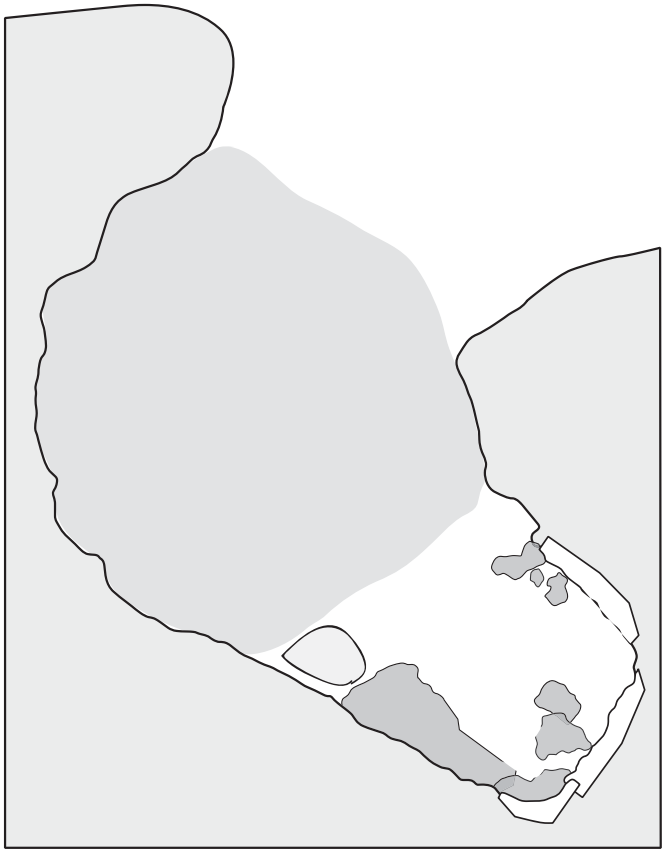

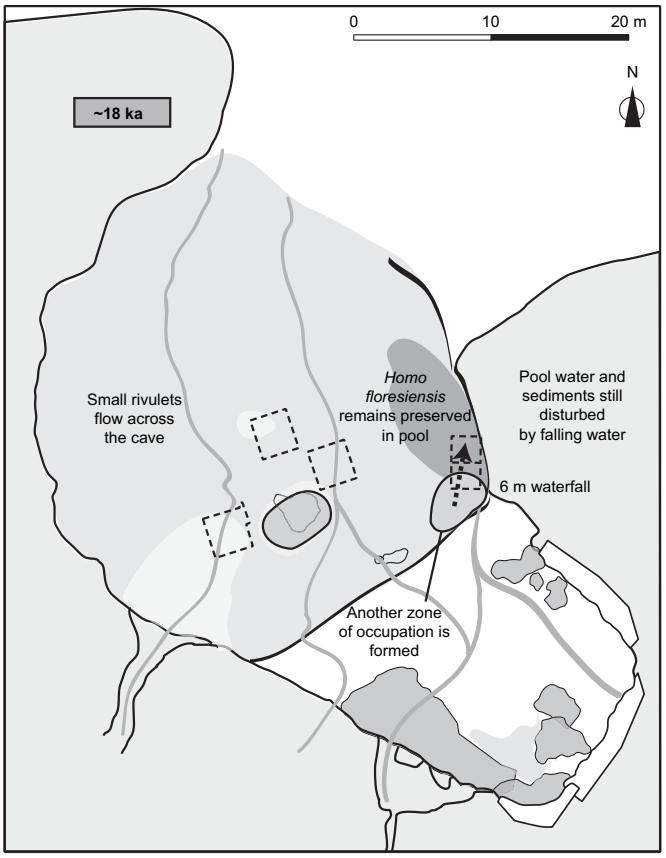

Figure 13. A schematic representation of the geomorphic evolution of Liang Bua at ~18 ka as a "time slice" showing the creation of a new zone of occupation in Sector XI. The pool by the east wall was maintained throughout this period, supplied by the east waterfall, which had substantially reduced in height due to sedimentary infilling.

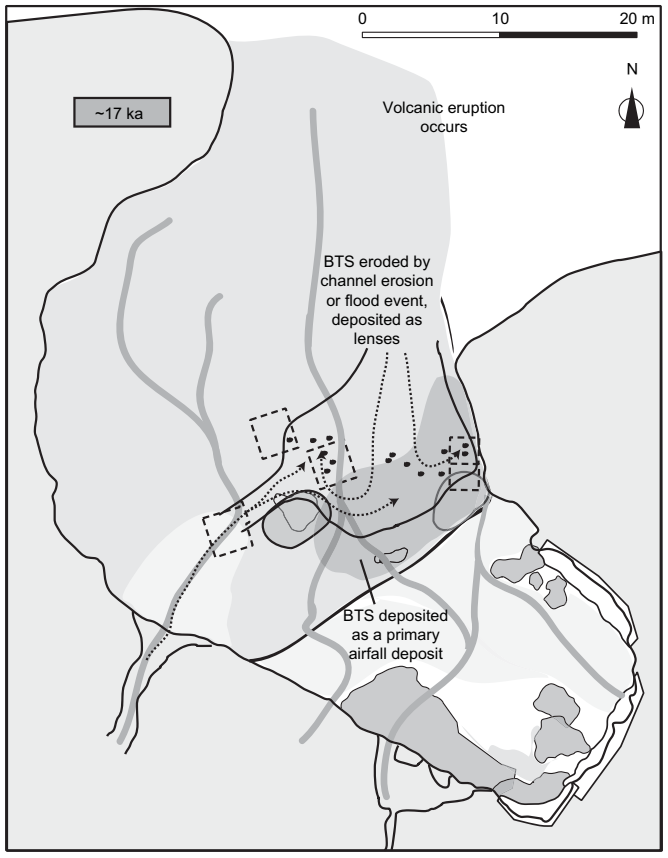

Figure 14. A schematic representation of the geomorphic evolution of Liang Bua at ~17 ka showing the deposition of the BTS unit (light black shading) and its subsequent removal (thick black line). A significant proportion of this unit was eroded by either channel erosion from Liang Tanah or a large flood event (dotted arrows), but individual lenses (filled black dots) were deposited within some of the sectors.

increase in the velocity of slope wash, resulting from a severe monsoon season that combined with the effects of gravity to rework the rounded cobbles. This deposition occurred in at least two phases, the oldest of which is represented by an age of 41 ± 10 ka (sample LBS7-46).

The occupation level containing the skeleton The pool by the east wall persisted in the cave environment for at least 40 k.yr., from 55 ± 8 ka (sample LBS7-45) to 11 cal. ka BP (sample ANUA-19211), and is represented in the sediments of Sector VII to thickness of at least 6 m. Throughout most of this period, the absence of sedimentary structures suggests that either the pool varied in depth, or the rear sinkholes and resulting waterfall (now reduced to ~6 m in height) was a source of intermittent disturbance and sedimentary infilling. The presence of a pool at this time is one of the reasons for the excellent preservation of the skeletal evidence, as once emplaced it was rapidly covered in fine silts during a period of channel inactivity. This sedimentary unit has been well constrained by radiocarbon and luminescence dating techniques. The calibrated ^{14}C age of 18 cal. ka BP from charcoal (samples ANUA-27117 and ANUA-27116) has been successfully bracketed by minimum age estimates of 14 ± 2 ka and 6.8 ± 0.8 ka from IRSL dating of feldspars (samples LBS7-40 and LBS7-42, respectively), and maximum age estimates of 40 ± 8 ka and 36 ± 5 ka from the DAP red TL dating of quartz (samples LBS7-40 and LBS7-42, respectively). These results predict that the burial of the skeleton occurred between 36–14 ka, which agrees with the ^{14}C result.

The southern half of Sector XI contains an area of higher ground, as suggested by the sloping deposits, the evidence of minor slumping, and the *in situ* location of the *Homo floresiensis* skeleton (Morwood et al., 2004, 2005). This area represents the bank deposits of the pool and a zone of occupation ~18 cal. ka BP (samples ANUA-27117 and ANUA-27116). The presence of flaking floors (Moore et al., 2009) suggests that this area was relatively flat and was the source for the occupational evidence found in Sector VII. Sector IV also displays evidence of occupation at this stratigraphic level, with a high concentration of artifacts that may have originated from the zone of occupation that had been established at ~74–61 ka. During the younger occupation period, at ~18 ka, the two other main channels in the cave may have been reduced to smaller rivulets, accompanied by the precipitation of large sheets of flowstone by the Liang Tanah passage and the southwest corner of Sector IV (Fig. 13). At 17 ka, this reduction in channels came to an abrupt end due to invigorated surface wash and channel processes. The timing of this change correlates with increases in precipitation according to climate records from the region (Westaway et al., 2009a).

At this stratigraphic elevation in Sector VII, the discovery of burnt stones arranged in a hearth (sample LBS7-44), provides evidence for fire use by *Homo floresiensis*. Although these stones proved difficult to constrain with TL techniques (Roberts et al., 2009), a minimum age of 22 ± 5 Gy for the faded feldspar signal, combined with the age of ~55 ka for the sediment in which they

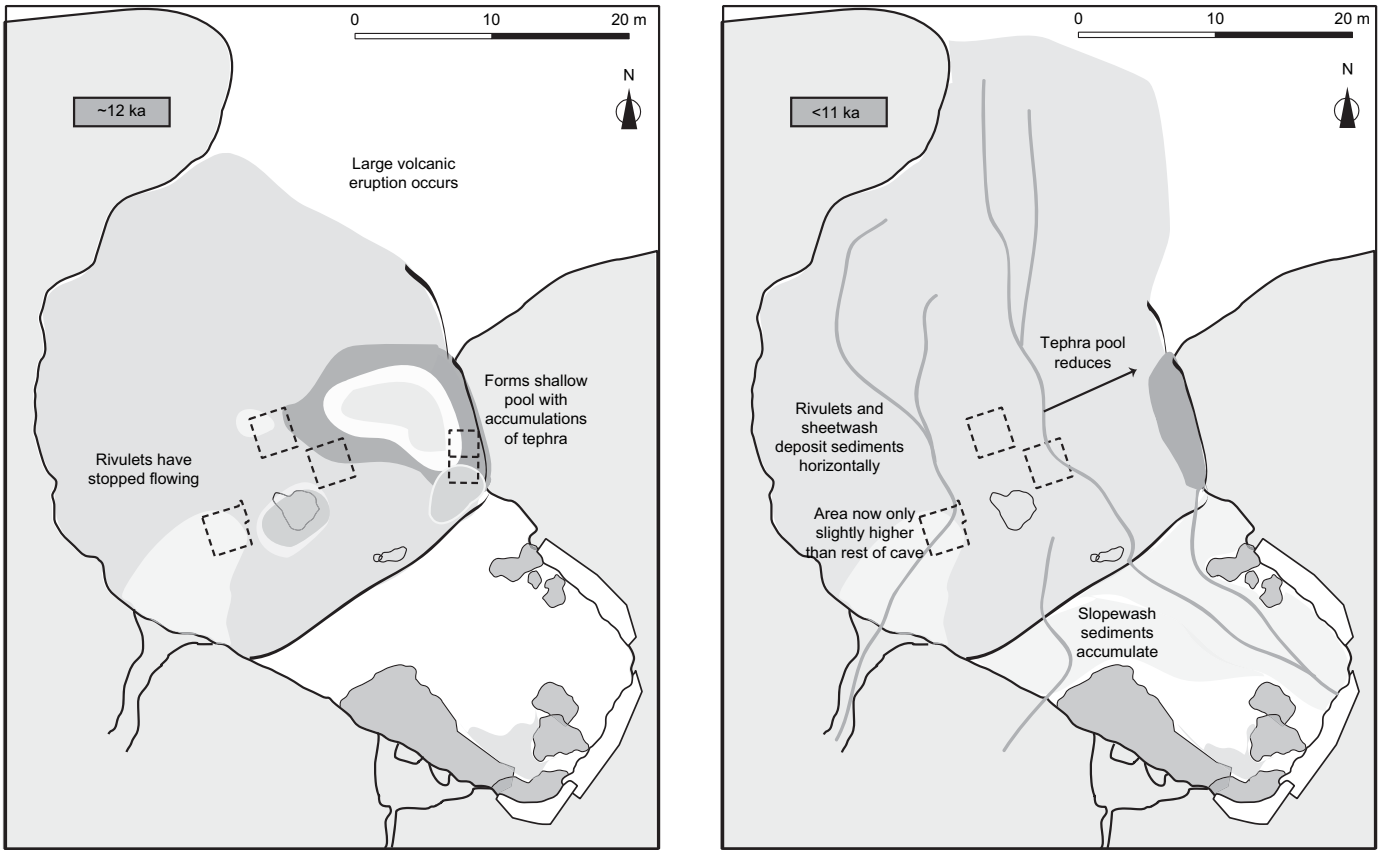

Figure 15. A schematic representation of the geomorphic evolution of Liang Bua at ~12 ka as a "time slice" showing the creation of a large, but shallow tephra pool, which stretched from the east wall to the center of the cave. During this time, all of the channels and many of the smaller rivulets stopped flowing, allowing the silts in the pool to settle and form fine laminations.

were found (sample LBS7-45) provides a useful indication for the timing of fire use in the cave.

Volcanic sediments Between ~18 ka (19.0–17.9 ka sample ANUA 27116) and 17 ka (17.1–15.8 ka sample ANUA 19203), the black volcanic sand unit (BTS) was deposited in the channel by the east wall (Fig. 14). The sharp lower bedding contact indicates that extensive erosion occurred within the channel prior to deposition. From the lack of sedimentary structure, degree of sorting and mafic composition, the BTS represents a primary airfall deposit from a localized eruption (Turney, pers. comm.) It is possible that this unit was broadly deposited and stretched from the east wall to the center of the cave, but an extensive sequence of erosion after ~17 ka removed a large section of this deposit and carved a deep ~2 m channel in the underlying unit that can be observed in Sectors XI, VII, III, and IV (Fig. 14). The source of this erosion may have been from increased channel activity from the Liang Tanah passage or from an external influence, such as an extreme flood event from the river that was situated ~10 m below the cave entrance at ~17 ka (Westaway et al., 2009a).

Infilling of this deep channel, in the form of consolidated lenses of the eroded BTS deposit, was initiated between 16–14 ka (17.1–15.8 ka sample ANUA 19203, 14 ± 3 ka sample LBS4-30) when the channels that had flowed through the cave since ~100 ka were transformed into a large pool. The sedimentology suggests that this body of water was an amalgamation of the pool that preserved the *Homo floresiensis* remains by the east wall and the other two channels, and extended to the middle of the cave across Sector IV and the edge of Sector III.

Within the next ~5 k.yr., between 13–11 cal. ka BP (samples ANUA-27115 and ANUA-19211), the pool acted as a sink for accumulating tephra deposits (WTS) from an extensive volcanic eruption that occurred between 12–11 ka. The presence of one large pool rather than a few, separate pools is suggested by: 1) the presence of similar tephra layers at the same depth (4 m) in Sectors VII and IV; 2) a similarity in the sedimentary characteristics of these layers, including loaded bedding structures and laminations; and 3) the presence of thin accumulations of these deposits in Sector III that represent the outer edge of the pool. After the initial deposition of the slightly coarser sandy silt unit, the pool deposits contained sedimentary structures (e.g., fine laminations) that imply little disturbance occurred during their deposition. In Sectors VII and IV, the correlation between the silt layering at these different ends of the pool also agrees with a reduction in water motion, but the greatest definition in the laminations is found in Sectors VII/XI, suggesting less motion occurred by the east wall than in the center of the cave. Thus, during the later part of pool evolution, this reduced motion implies that the waterfall by the east wall had temporarily dried up. In addition, the absence of channel deposits at this stratigraphic elevation implies that the other two channels had also ceased to operate (Fig. 15). The BTS and WTS units are important stratigraphic markers for correlation purposes, and are associated with the extinction of *Stegodon* in this cave.

The younger occupation layers and modern slope wash The sedimentology of the youngest sediments within the cave suggests that by the early Holocene, at ~10 cal. ka BP (samples ANUA-19206, ANUA-19211, and ANUA-19207), the pools and channels had disappeared. Likewise, sheetwash replaced rill wash and overland flow, resulting in the horizontal deposition of clayey silts. This change in the dominant cave processes removed the uneven topography and created a level cave-floor surface that was better suited to occupation. Accordingly, this change corresponds to an intensification of site occupation, when artifacts, charcoal, and bone concentrations rapidly increased (Morwood et al., 2004, 2005, 2009) between ~10–2 ka (samples ANUA-19211 and WK-16353). In Sector I, the upper layers of this unit are interspersed with thin layers of flowstone, suggesting that the passage from Liang Tanah was still channelling water into the cave. During this period, the floor of the front chamber reached a similar level as the rear, causing the two chambers to coalesce. In addition, the rear chamber developed steep slope wash accumulations from the periodically active rear sinkhole (Fig. 16), and caused the cave environment to evolve into its present-day form.

The sedimentology of Liang Bua: a regional context

The deposits at Liang Bua provide a unique and relatively well-preserved 100 k.yr. sequence of sedimentary, faunal, and archaeological change on Flores. The interbedded and complex nature of its layers demands a thorough understanding of the stratigraphic relationships to unravel the history of the site. It is the combination of deep excavation, an understanding of the environmental context (see Westaway et al., 2009), use of geomorphological and sedimentological techniques, and the application of a wide range of dating methods (see Roberts et al., 2009) that was crucial to this research and provides the greatest methodological advance for cave site analysis in Southeast Asia.

Liang Bua has many geomorphological and stratigraphic parallels with other large excavated caves in this region, e.g., distinct sequences of interbedded deposits with a weak age/depth relationship (Gilbertson et al., 2005), and the dominance of diagenetic and karstic processes (Glover, 1979; Gilbertson et al., 2005). Liang Bua also contains evidence of sediment accumulation in large basins (Units 3, 8, and 9), which is a depositional trait in Niah Cave, Sarawak (Gilbertson et al., 2005). In addition, it shows rapid and variable sediment accumulation influenced by sinkhole action, as observed in Ulu Leang and Leang Burung II in Sulawesi (Glover, 1979, 1981) and Toe Cave in Papua (Pasveer et al., 2002). Sediment deposition at Niah, Ulu Leang, and Long Rongrien (Thailand) have also been heavily influenced by fluvial action and modified by episodes of reworking (Glover, 1979; Anderson, 1997; Gilbertson et al., 2005).

In contrast, the sediments in the caves previously mentioned have suffered from the effects of bioturbation, especially guano deposition (Glover, 1979; Anderson, 1997; Gilbertson et al., 2005), whereas the stratigraphy of Liang Bua displays very little biological disturbances. Deposits at Ulu Leang and Leang Burung have also heavily subsided (Glover, 1979, 1981), whereas those at Liang Bua display only minor sink erosion and subsidence in the basal layers, which has not disturbed the relatively clear lithostratigraphy. This relative stability, combined with the capping flowstone and conglomerate layers, has helped preserve the occupational evidence.

Summary

An analysis of the main sedimentary units in Liang Bua has enabled a reconstruction of the geomorphic and sedimentary history of the cave during the time of hominin occupation. A sedimentological analysis of these units has identified a sequence of geomorphological events that may have restricted occupation to certain zones. This sequence confirms the maximum age of occupation ~190 ka, but suggests that continuous occupation of the cave may not have been possible until after ~100 ka, when the accumulated water had drained from the front chamber. The next ~89 k.yr. were dominated by flowing water (in the form of slope and surface wash) creating waterfalls, cut-and-fill by channels, periodic pooling of water, and occasional volcanic events. In amongst these geomorphological and sedimentological changes, and directed by the location of higher ground, at least three zones of occupation may have existed: two earlier zones established ~74–61 ka and located by the west wall and center of the cave (to the southwest of Sector IV and the southwest corner of Sector I), and a later zone established ~18 ka and located by the east wall (to the south of Sectors VII and XI). The identification, timing, and location of these zones provides a depositional context for the archaeological evidence found at Liang Bua, and demonstrates the value of reconstructing the geomorphic history of archaeological sites in this region.

Acknowledgements

This study was funded by a Discovery Project grant to M.J.M. from the Australian Research Council (ARC), with additional funding to R.G.R. from the University of Wollongong. We also thank the ARC for a Senior Research Fellowship to R.G.R.; T. Dubiantono and colleagues at the Center for Archaeology (Jakarta) for logistical support in Flores and Java; T. Lancaster, Ginardo and Pa Teguh for field assistance; and P. Westaway and the University of Wollongong (University Postgraduate Award and Tuition Fee-Waiver Scholarship) for financial support of K.E.W.

References

Anderson, D.D., 1997. Cave archaeology in Southeast Asia. Geoarchaeology 12, 607–638.
Bridge, J.S., 2003. Rivers and Floodplains: Forms, Processes and Sedimentary Record. Blackwell., Oxford.
Carr, P.F., Pemberton, J.W., Nunan, E., 1999. Low-grade metamorphism of mafic lavas, Late Permian Broughton Formation, Sydney Basin. Aust. J. Earth Sci. 46, 839–849.
Chivas, A.R., Garcia, A., van der Kaars, S., Couapel, M.J.J., Holt, S., Reeves, J.M., Wheeler, D.J., Switzer, A.D., Murray-Wallace, C.V., Banerjee, D., Price, D.M., Wang, S.X., Pearson, G., Edgar, N.T., Beaufort, L., De Deckker, P., Lawson, E., Cecil, C.B., 2001. Sea-level and environmental changes since the last interglacial in the Gulf of Carpenteria, Australia: an overview. Quatern. Int. 83–85, 19–46.
Gardiner, V., Dackombe, R. (Eds.), 1983. Geomorphological Field Manual. George Allen and Unwin, London.
Glover, I.C., 1979. The effects of sink action on archaeological deposits in caves: An Indonesian example. World Archaeol. 10, 302–317.
Glover, I.C., 1981. Leang Burung 2: an upper Palaeolithic rock shelter in South Sulawesi, Indonesia. Mod. Quat. Res. SE Asia 6, 1–38.
Gilbertson, D., Bird, M., Hunt, C., McLaren, S., Mani Banda, R., Pyatt, B., Rose, J., Stephens, M., 2005. Past human activity and geomorphological change in a guano-rich tropical cave mouth: initial interpretations of the Late Quaternary succession in the Great Cave of Niah, Sarawak. Asian Perspect. 44, 16–41.
Moore, M.W., Sutikna, T., Jatmiko, Morwood, M.J., Brumm, A., 2009. Continuities in stone flaking technology at Liang Bua Cave, Flores, Indonesia. J. Hum. Evol. 57 (5), 503–526.
Morwood, M.J., Soejono, R.P., Roberts, R.G., Sutikna, T., Turney, C.S.M., Westaway, K.E., Rink, W.J., Zhao, J-x., van den Bergh, G.D., Rokus Awe Due, Hobbs, D.R., Moore, M.W., Bird, M.I., Fifield, L.K., 2004. Archaeology and age of a new hominin from Flores in eastern Indonesia. Nature 431, 1087–1091.
Morwood, M.J., Brown, P., Jatmiko, Sutikna, T., Saptomo, E.W., Westaway, K.E., Rokus Awe Due, Roberts, R.G., Maeda, T., Wasisto, S., Djubiantono, T., 2005. Further evidence for small-bodied hominins from the Late Pleistocene of Flores, Indonesia. Nature 437, 1012–1017.
Morwood, M.J., Sutikna, T., Saptomo, E.W., Jatmiko, Hobbs, D.R., Westaway, K.E., 2009. Preface: Research at Liang Bua, Flores, Indonesia. J. Hum. Evol. 57 (5), 437–449.
Pasveer, J.M., Clarke, S.J., Miller, G.H., 2002. Late Pleistocene human occupation of inland rainforest, Bird's Head, Papua. Arch. Oceania 37, 92–95.
Roberts, R.G., Westaway, K.E., Zhao, J.-x, Turney, C.S.M., Bird, M.I., Rink, W.J., Fifield, L.K., 2009. Geochronology of cave deposits at Liang Bua and of adjacent river terraces in the Wae Racang valley, western Flores, Indonesia: a synthesis of age estimates for the type locality of *Homo floresiensis*. J. Hum. Evol. 57 (5), 484–502.

Shahack-Gross, R., Berna, F., Karkanas, P., Weiner, S., 2004. Bat guano and preservation of archaeological remains in cave sites. J. Archaeol. Sci. 31, 1259–1272.

Westaway, K.E., 2006. Reconstructing the Quaternary landscape evolution and climate history of western Flores: an environmental and chronological context for an archaeological site. Ph.D. Dissertation, University of Wollongong.

Westaway, K.E., Morwood, M.J., Roberts, R.G., Zhao, J.-x., Sutikna, T., Saptomo, E.W., Rink, J., 2007. Establishing the time of initial human occupation of Liang Bua, western Flores, Indonesia. Quatern. Geochronol. 2, 337–343.

Westaway, K.E., Roberts, R.G., Sutikna, T., Morwood, M.J., Drysdale, R., ZhaoJ.-x, Chivas, A.R., 2009a. The evolving landscape and climate of western Flores: an environmental context for the archaeological site of Liang Bua. J. Hum. Evol. 57 (5), 450–464.

Westaway, K.E. Morwood, M.J., Sutikna, T., Moore, M.W. Rokus, A.D., van den Bergh, G.D., Roberts, R.G., Saptomo, E.W., 2009b. *Homo floresiensis* and the Late Pleistocene environments of eastern Indonesia: defining the nature of the relationship. Quatern. Sci. Rev., in press.